GIScience & Remote Sensing

ISSN: (Print) (Online) Journal homepage: https://www.tandfonline.com/loi/tgrs20

In situ hyperspectral characteristics and the discriminative ability of remote sensing to coral species in the South China Sea

Kai Zeng, Zhantang Xu, Yuezhong Yang, Yongming Liu, Hongwuyi Zhao, Yu Zhang, Baicheng Xie, Wen Zhou, Cai Li & Wenxi Cao

To cite this article: Kai Zeng, Zhantang Xu, Yuezhong Yang, Yongming Liu, Hongwuyi Zhao, Yu Zhang, Baicheng Xie, Wen Zhou, Cai Li & Wenxi Cao (2022) *In situ* hyperspectral characteristics and the discriminative ability of remote sensing to coral species in the South China Sea, GIScience & Remote Sensing, 59:1, 272-294, DOI: 10.1080/15481603.2022.2026641

To link to this article: https://doi.org/10.1080/15481603.2022.2026641

Published online: 13 Jan 2022.

GISCIENCE & REMOTE SENSING
2022, VOL. 59, NO. 1, 272–294
https://doi.org/10.1080/15481603.2022.2026641

In situ hyperspectral characteristics and the discriminative ability of remote sensing to coral species in the South China Sea

Kai Zeng[a,b], Zhantang Xu[a,c,d], Yuezhong Yang[a,c], Yongming Liu[a,c,d], Hongwuyi Zhao[a,b], Yu Zhang[a,b], Baicheng Xie[a,b], Wen Zhou[a,c,d], Cai Li[a,c] and Wenxi Cao[a,c]

[a]State Key Laboratory of Tropical Oceanography (LTO), South China Sea Institute of Oceanology, Chinese Academy of Sciences, Guangzhou, China; [b]University of Chinese Academy of Sciences, Beijing, China; [c]Southern Marine Science and Engineering Guangdong Laboratory (Guangzhou), Guangzhou, China; [d]Guangdong Key Lab of Ocean Remote Sensing, Guangzhou, China

ABSTRACT

Knowledge about the optical features of benthic objects is essential for quantifying spectral signatures, remote sensing-based mapping, and ecological monitoring in coral reefs. However, the spectral identification of benthic species and the accurate measurement of the *in situ* reflectance spectra of relevant research objects remain underexplored. An underwater radiation measuring system suitable for coral reef environments was specifically designed to obtain *in situ* reflectance spectra and match benthic photographs of various substrate targets. This instrument has the advantages of obtaining hyperspectral, dual-channel simultaneous measurements, and automatically adjusting the integration time according to the light intensity. Based on *in situ* hyperspectral datasets, the linear discriminant analysis (LDA) was used for exploring and discriminating spectral characteristics from three taxonomic ranks, which include typical substrates of six community groups, nine coral families, and six *Acroporidae* species. *In situ* full-resolution (1-nm) spectra provided the best discrimination ability with mean accuracies of 97.5%, 90.9%, and 91.6% for typical substrates, coral families, and coral species, respectively. The spectral abilities of remote sensors were assessed by applying the spectral response functions of three multispectral sensors (Landsat 8 OLI, Sentinel-2A, and World View-2) to the full-resolution spectra. Discrimination analyses of the simulated spectra demonstrated that the spectral separations of typical substrates might be apparent, with overall classification accuracies of 89.6%, 88.2%, and 90.4% for the Landsat 8 OLI, Sentinel-2A, and World View-2 sensors, respectively. The spectral separation for different corals, however, may not be effective when using multispectral sensors. The discrimination analyses of families and species produced overall classification accuracies of 67.1% and 69.6%, respectively, for the Landsat 8 OLI, 56.0% and 56.0% for the Sentinel-2A sensor, and 64.5% and 61.8% for the World View-2 sensor. In summary, this method has the potential for identifing substrate targets in communities and taxonomic coral groups by applying *in situ* hyperspectral datasets. Furthermore, multispectral satellite sensors are currently inadequate for spectrally separate corals, while spectral discrimination is possible and practical for different substrate targets with visual spectral differences.

ARTICLE HISTORY
Received 24 August 2021
Accepted 29 December 2021

KEYWORDS
Coral reef; discrimination; hyperspectral; sea-bottom reflectance; remote sensing

1. Introduction

Coral reef ecosystems are among the most biologically diverse ecosystems and serve as essential habitats and refuges for various fish and shellfish species (Knudby, LeDrew, and Newman 2007). Hyperspectral remote sensing has recently attracted much attention to the quantification of spectral signatures, the mapping of geomorphic zones, and to the identification of temporal changes in coral reef habitats (Mumby et al. 1998; Klemas 2011; Hedley et al. 2012; Garcia, Lee, and Hochberg 2018; Gapper et al. 2018; Li et al. 2020). *In situ* reflectance measurements and characteristic spectral identifications of various benthic communities bridge the gap between laboratory measurements and remote sensing (Karpouzli, Malthus, and Place 2004). Analyses of *in situ* spectral data can be used to determine optimal bandwidths and appropriate spectral resolutions with which to discriminate substrate targets for remote sensing applications in studies of coral reefs (Hochberg and Atkinson 2003).

Each benthic material presents a characteristic reflectance (Karpouzli and Malthus 2003; Kutser, Dekker, and Skirving 2003). As a function of the substrate structure and material composition (Lyzenga 1978; Maritorena, Morel, and Gentili 1994), this

CONTACT Zhantang Xu xuzhantang@qq.com

reflectance represents the signal reflected from the sea bottom in the radiative transfer process (Kazama and Yamamoto 2017). Multiple studies of spectral characteristics have indicated that it is possible to spectrally discriminate among several fundamental reef benthic communities, such as coral, bleached coral, seagrass, algae, and sand (Holden and LeDrew 1998; Kutser et al. 2001; Hochberg, Atkinson, and Andréfouët 2003; Karpouzli, Malthus, and Place 2004; Idris, Jean, and Zakariya 2009). However, some spectral feature differences exist among different studies, and it is challenging to create a global spectral database by integrating data from various studies. One of the reasons this is difficult is that no unified reflectance measurement norms or specifications exist.

There are four main ways to obtain sea-bottom reflectance measurements. First, benthic samples can be sampled in the air for reflectance measurements or measured under cultivation conditions in the laboratory (Hardy et al. 1992; Hedley et al. 2004; Russell et al. 2016). For example, Maritorena, Morel, and Gentili (1994) published the reflectance spectra of multiple types of algae and coral sand measured in the laboratory. Although the effects of the water column can be avoided in such measurements and the sample conditions can be controlled conveniently and flexibly, the measurements obtained using this method may not realistically represent the reflectance of the benthic substrates for a given observation due to natural variabilities and the destruction of the original light field. The reflectances measured in the laboratory may lack the practical application significance of natural environmental conditions. Second, reflectances can be obtained by correcting the influence of the water column on the water surface (Karpouzli, Malthus, and Place 2004; Caras and Karnieli 2013; Miller et al. 2016). Not only the air–water interface correction will introduce error by the complexity of surface waves, but also the water column correction will introduce uncertainty since the rapidly changing underwater light field in coral reefs. Therefore, the superposition of the above double errors will lead to great uncertainty and even unavailability of data. Significantly, some uncontrollable factors, such as sea waves and the underwater mixing process, cause the aquatic light field to change rapidly (Ackleson 2003). Variations in water depths, the reflectance features of the substrates, and the optical properties of the water column can contribute complexity to the interpretation and identification of substratum information (Mishra et al. 2007). Third, some researchers have calculated reflectances by measuring the upwelling and downwelling radiant fluxes underwater through the use of one or two radiometer probes (Holden and LeDrew 1997; Wettle et al. 2003; Idris, Jean, and Zakariya 2009). Noticeably, the absorption and attenuation effects of the water column are inconsistent between the upward and downward optical paths if the two radiant flux measurements are not set at the same level with the same optical path lengths. Furthermore, the influence of instrument self-shadowing and the inconsistent light field caused by rapid changes in the underwater light field lead to errors. Fourth, some measurements have been carried out *in situ*, with incident irradiance values obtained using diffuse reflectors (Hochberg and Atkinson 2000; Kutser, Dekker, and Skirving 2003; Leiper, Phinn, and Dekker 2012; Roelfsema and Phinn 2012). The calibration accuracy of the reflected panel determines the accuracy of this method. Overall, *in situ* observations of the characteristic reflectance parameters are required to develop, refine, and validate remote sensing algorithms. The accurate collection of *in situ* sea-bottom reflectances requires designing an underwater radiation measuring system that is suitable for the complex aquatic environments of coral reefs.

Although many studies on reflectance characteristics have revealed the spectral separability of different substrate materials such as coral, bleached coral, seagrass, algae, and sand (Holden and LeDrew 1998; Kutser et al. 2001; Hochberg, Atkinson, and Andréfouët 2003; Karpouzli, Malthus, and Place 2004), these studies have focused on limited numbers of species and regional scopes. In addition, few of these previous studies determined whether corals are (or are not) separable at the species level (Torres-Perez, Guild, and Armstrong 2012; Russell et al. 2016). Instead, corals have been separated into coarse groups including three main optical types: green, blue, and brown corals (Hochberg, Atkinson, and Andréfouët 2003; Hochberg et al. 2004; Karpouzli, Malthus, and Place 2004). Alternatively, some studies have dealt with habitat classes created by using cluster analyses of the spectral angles of field data (Holden and LeDrew 1998). A few previous studies have been devoted to the taxonomy spectral

identification of coral species (Kutser and Jupp 2006; Stambler and Shashar 2007; Idris, Jean, and Zakariya 2009; Russell et al. 2016). Kutser and Jupp (2006) used a cluster analysis and derivative analysis to test the possibility of discriminating *Acropora* at the species level and showed that it is challenging to recognize corals at the genus level. Nevertheless, the practical applications of spectral separability and the discrimination of the reflectance features of benthic communities remain underexplored.

Theoretically, it is possible to collect a hyperspectral library that contains all possible water depths and reflectance spectra of all potential substrate targets (Mobley et al. 2005). Then, the water depth and bottom type could be simultaneously retrieved utilizing spectral matching technology (Maritorena, Morel, and Gentili 1994; Mobley 1994; Gege 2004, 2014). Some analysis methods have been established based on premodeled spectral libraries (Mobley et al. 2005; Kutser, Miller, and Jupp 2006; Lesser and Mobley 2007). These libraries include the reflectance spectra of different substrate targets at different water depths. A model containing the complexity of benthic structures has been designed (Hedley et al. 2016), but this model has not been used in mapping applications. The detailed spectral characteristics of benthic communities and the underwater radiative transfer process are still serious aspects restricting the accurate extraction of information regarding coral reefs. Limited by the *in situ* measurement data available for comparisons and verifications, the water column correction algorithms that have been established to retrieve substrate information have not been applied effectively (Barnes et al. 2013; Chen et al. 2019; Niroumand-Jadidi, Pahlevan, and Vitti 2019). *In situ* measurement data of the sea-bottom reflectances of coral reefs are an essential and urgent need for remote sensing monitoring research. Data with higher spectral resolutions significantly enhance the classification capability to increased depths or to the same depths in more turbid water columns (Botha et al. 2013). Developing effective strategies and measurement tools for collecting and utilizing *in situ* observations are essential if remote sensing is to be advanced as a central tool for research and applications in coral reef regions.

The goals of our work were to (1) design and build an accurate reflectance-measuring system to obtain *in situ* sea-bottom hyperspectral data; (2) classify and document the spectral features of different corals, coral debris, seagrasses, sands, and other sediments distributed within the Sanya coastal region and Xisha Islands in the South China Sea; and (3) establish the sea bottom spectral datasets in the South China Sea and evaluate the discriminative abilities of the remote sensors at the species taxonomic level. This research provides baseline information on the optical characteristics of different benthic communities and promotes the hyperspectral identification and distinguishing of some coral species.

2. Study area

The South China Sea is rich in hermatypic coral species, accounting for almost 1/3 of the number of species worldwide, and the South China Sea Islands and Hainan Island are the main distribution areas of these corals (Zhao, Yu, and Zhang 2006). The Xisha Islands has a complete ecosystem structure that is mainly covered with sand, coral reefs, and seagrass (Huang, Dong, and Lian 2008). The Sanya coastal region, located at the southernmost part of Hainan Island, represents a critical ecological zone among tropical coastal ecosystems and the Sanya Coral Reef National Nature Reserve has been established in this region. Our measurements were carried out in coral reef areas with depths of less than 20 m along the Sanya coast (18°06′–18°45′ N, 109°20′–110°36′ E) and Xisha Islands (15°46′–17°08′ N, 111°11′–112°54′ E) in September 2018 and November 2018 (Figure 1).

3. Methods

3.1 In situ *sea-bottom reflectance collection*

The *in situ* reflectance spectra of the different habitats and species were measured using a self-designed, dual-beam sea-bottom reflectance measuring instrument. The device integrates two spectral channels, which simultaneously measure the incident and reflected radiation fluxes of underwater benthic objects. The basic measurement principles are as follows.

The spectral reflectance R is defined as the ratio of the reflected radiant flux to the incident radiant flux (Morel and Smith 1982). In this paper, $R(z)$ is the fraction of downward irradiance, $E_d(z)$, that is reflected by the different bottom-types, $E_u(z)$, at depth z just above the bottom surface (Mobley 1994)

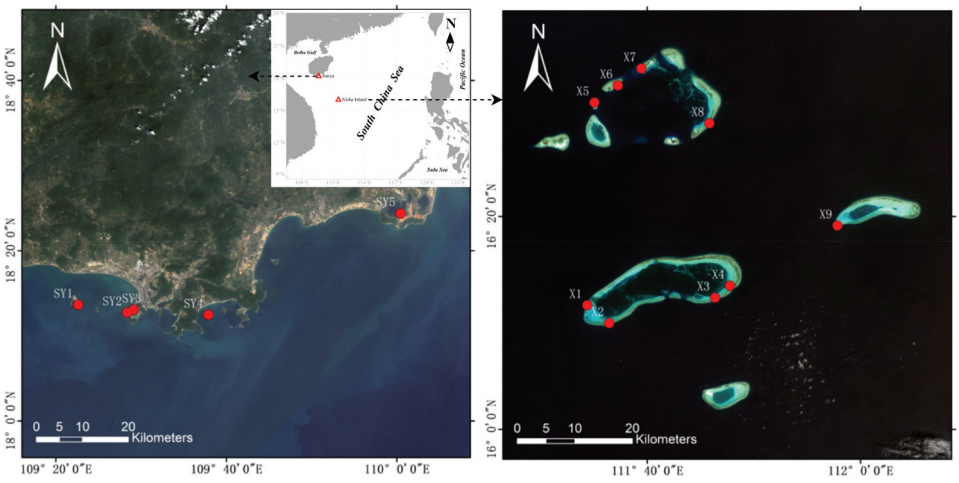

Figure 1. Study area of the Sanya coast and Xisha Islands in the South China Sea and the locations of the *in situ* study sites.

$$R(z) = \frac{E_u(z)}{E_d(z)} \tag{1}$$

For coral reef benthos, z is the depth of the substrate, and R is the fraction of light that is reflected upward by the surfaces of the reef benthos.

The relationship between the incident spectral irradiance, E_i, and the spectral radiance, L_r, reflected by a Lambertian panel is as follows:

$$E_i(z) = \pi \cdot L_r(z) \tag{2}$$

The downwelling radiant flux was measured via the reflected radiant flux from a calibrated diffuse white Spectralon panel; this method differs from the method in which direct measurements of the upwelling and downwelling radiant fluxes are used to calculate the reflectance. By regarding this panel as Lambertian with a known reflectance and combining Equations 1 and 2, the expression of the downwelling irradiance, $E_d(z)$, can be obtained:

$$E_d(z) = \frac{\pi \cdot L_0(z)}{\rho} \tag{3}$$

where ρ is the reflectance of the calibrated diffuse Spectralon panel; $L_0(z)$ is the reflected radiance from the whiteboard at depth z; and $E_d(z)$ is the underwater downwelling irradiance at depth z.

To obtain accurate reflectances, the ambient light fields of both the substrate and the diffuse whiteboard must be the same during the reflected radiation measurements. First, the distance between the probe and the target should be as close as possible to reduce the absorption and attenuation of the water column. Second, the reflected radiation of the two probes must be measured simultaneously to avoid errors caused by rapid light field changes. Finally, the measured positions, distances, and view angles of the two probes need to be set to the same values and synchronized to control the two optical channels with the same optical-environmental conditions. The measurement result is valid and representative through the elimination of the influence of the water between the probe and the substrate.

Treating benthic objects as Lambertian, the reflectance of the substrate target is expressed as follows:

$$R(z) = \rho \cdot \frac{\int_0^{2\pi}\int_0^{\frac{\pi}{2}} L_u(z,\theta,\emptyset)\cos\theta\sin\theta d\theta d\emptyset}{\pi \cdot L_0(z)} \tag{4}$$

where $L_0(z)$ and $L_u(z, \theta, \phi)$ are the reflected radiance of the diffuse whiteboard and substrate target measured by a two-channel spectrometer, respectively; θ is the underwater solar zenith angle; and ϕ is the underwater viewing azimuth angle with respect to the solar plane.

Figure 2(a) shows a diagram of the sea-bottom reflectance measurement system. The system collects the radiant fluxes of the two channels and the matching target image synchronously. The software can adjust the integration time automatically to determine the optimum light accepted by the sensors according to the radiation intensity at the scene. The *in situ* reflectance measurement is also automatic, except the orientation and distance, which need to be controlled manually during underwater measurements. The optical channel was an Ocean Optics Maya2000 Pro spectrometer (Ocean Optics, Inc., USA) with an 85% quantization rate and

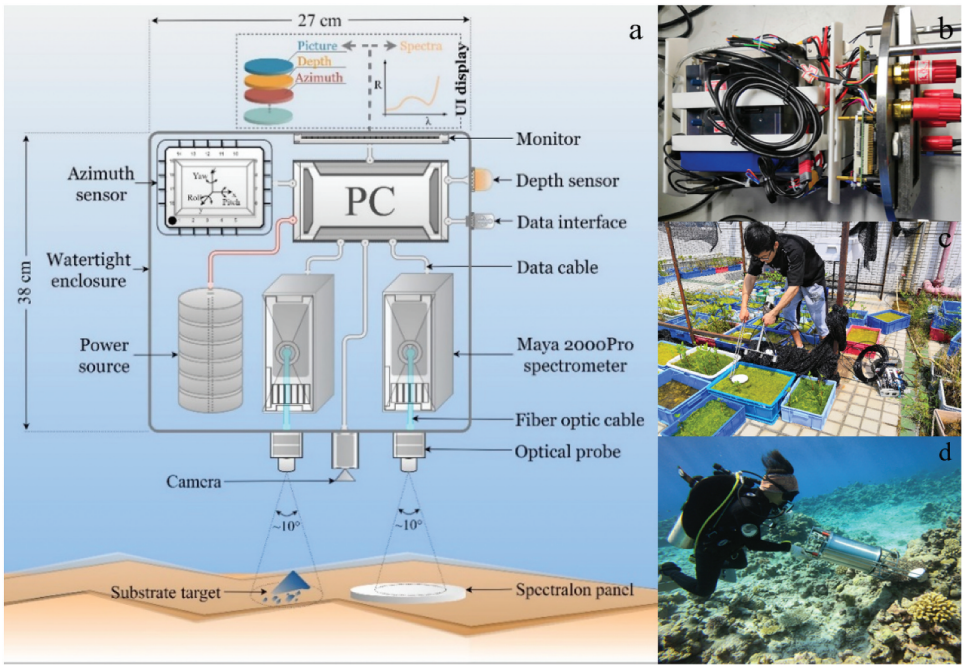

Figure 2. (a) Schematic diagram of *in situ* sea-bottom reflectance collection. (b) The internal structure of the instrument. (c) Laboratory examination. (d) Underwater field operation photograph.

a 0.3-m fiber optic cable (400 μm in diameter) with a full field view of ~10° fore-optic probe fitted to the optical fiber. The field of view (FOV) of the probe was limited to only that of the target to ensure that only pure endmember was collected (Hochberg and Atkinson 2000; Botha et al. 2013). This instrument was designed for portability and for conducting measurements over the range of 198 to 1120 nm with a sampling interval of ~0.5 nm and a full width at half-maximum resolution of ~3 nm. The equipped camera parameters are 1920 × 1080 resolution, a 95–100° field of view, and a frame rate of 30 fps.

Reflectance spectra were measured consistently at approximately 0.25 m above the substrate target to cover a specific target area with a FOV of about 4 cm diameter. At least five L_0 and L_u measurements were made within a 2-s sampling interval for each substrate target. Meanwhile, underwater photographs of each target were collected simultaneously for species identification and to obtain descriptions of the surrounding feature types and some other additional information. Furthermore, *in situ* reflectance spectra were measured and processed for visible wavelengths (400–700 nm, interpolated to 1-nm intervals) following the methods described in Zeng et al. (2020). The measurement azimuth angle was set to follow the technical regulations for ocean optical surveys (Mueller et al. 2003), and the self-shadowing influence of the instrument was avoided in the measurement process as much as possible. The reflectance data were collected during cloud-free days, with calm seas when the solar elevation angle was high (9:00 am–3:00 pm).

The sea-bottom reflectance at the depths more than 10 m has a signal absence at the red band, because of the strong absorption and attenuation effect of the water column. We created a spectral library of 1762 reflectance spectra of coral reefs with depths of less than 10 m and matching substrate images. This library encompasses 29 species of coral, one seagrass species, one seaweed species, five sand samples, three bleached coral species, a coral rubble sample, and some other sediment samples (Table 1). The coral species identification was conducted in reference to the World Coral Website (http://www.coralsoftheworld.org/page/home/) and the World Register of Marine Species (http://www.marinespecies.org/).

3.2 Spectral separability analysis

A significant part of emitted sunlight is in the visible region, while a small fraction is in the ultraviolet, and the strongest wavelengths absorbed by water are in

Table 1. Species reflectance spectra collected around the Sanya coast and Xisha Islands habitats.

Area	Feature	Family	Species	Number of spectra (N)
Sanya coast	Corals	*Acroporidae*	*Acropora cervicornis*	21
		Merulinidae	*Goniastrea edwardsi*	18
		Poritidae	*Porites lobata*	7
	Chlorophyta	*Derbesiaceae*	Unknown	35
	Seagrass	*Hydrocharitaceae*	*Enhalus acoroides*	38
	Sandy beach			57
	Sand mixed with gravel			45
	Fine-grained carbonate sand			10
	Sand mixed with silt			33
Xisha Islands	Corals	*Acroporidae*	*Acropora austera*	9
			Acropora cerealis	34
			Acropora cytherea	107
			Acropora humilis	14
			Acropora hyacinthus	78
			Acropora samoensis	31
		Dendrophylliidae	*Turbinaria radicalis*	27
		Diploastreidae	*Diploastrea heliopora*	20
		Fungiidae	*Ctenactis echinata*	47
		Lobophylliidae	*Acanthastrea echinata*	13
			Symphyllia radians	22
		Merulinidae	*Caulastraea echinulata*	10
			Leptastrea purpurea	28
			Leptoria phrygia	13
			Merulina ampliata	6
		Pocilloporidae	*Pocillopora damicornis*	10
			Pocillopora ligulata	26
		Poritidae	*Goniopora lobata*	22
			Porites cylindrica	174
			Porites densa	40
			Porites lutea	48
			Porites lobata	24
			Porites mayeri	23
		Siderastreidae	*Psammocora profundacella*	30
		Agariciidae	*Pavona varians*	22
			Pachyseris rugosa	30
	Sea anemone	*Actiniidae*	*Anthopleura nigrescens*	15
	Bleached coral	*Acroporidae*	*Acropora copiosa*	35
			Acropora grandis	27
		Pocilloporidae	*Pocillopora elegans*	16
	Coral reefs covered by the water column			151
	Coral rubble			96
	White attachment			156
	White sand			34
	White sand mixed with coral rubble			18
	White sand and water column			42
SUM				1762

the near-infrared. All spectra were processed over the visible region from 400 to 700 nm with linear interpolation to 1-nm intervals and smoothed in MATLAB (MathWorks, USA) with a Savitzky-Golay filter (Savitzky and Golay 1964) with a window size of 8 to improve the overall noise reduction. Figure 3 shows a flowchart of the spectral analysis methods used in this study.

3.2.1 Derivative spectroscopy

Derivative spectroscopy is a common method in hyperspectral data analyses (Demetriades-Shah, Steven, and Clark 1990; Karpouzli, Malthus, and Place 2004; Ruffin, King, and Younan 2008). The reflectance spectra of corals are similar but contain subtle features that may help distinguish different species. These subtle spectral features are easily separated by using derivative spectroscopy, which can amplify spectral details to improve the reflectance spectra detection sensitivity (Huguenin and Jones 1986). The process of creating derivative spectra was implemented with MATLAB proceeded using a finite approximation to calculate the change in reflectance over a bandwidth, $d\lambda$, and the nth derivative can be expressed as:

$$D^n(\lambda) = \frac{d^n A}{d\lambda^n} \tag{5}$$

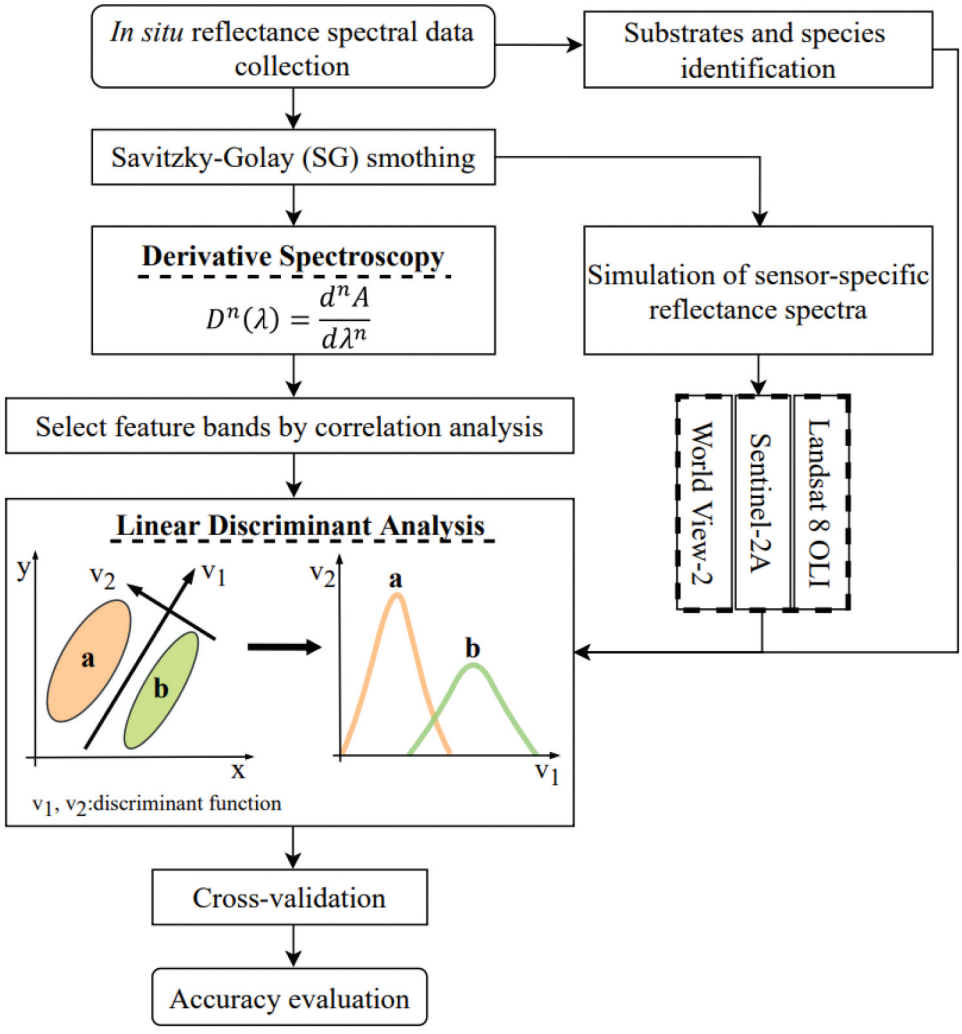

Figure 3. Flowchart outlining the framework of the spectral processing and analysis methods used in this study. Derivative spectroscopy and LDA were used to conduct a classification analysis of the class spectral separability of various substrate targets. Simulated reflectance spectra were used to evaluate the discriminative abilities of the multispectral satellite sensors.

where *n* is derivative order, $D^n(\lambda)$ represents the value of n-order derivative at analytical wavelength (λ).

3.2.2 Linear discriminant analysis

Linear discriminant analysis (LDA) was used to determine the best discriminating wavelengths, and a model was established to separate the substrate targets at three hierarchical levels: typical substrates representing the habitat scale, coral families, and coral species. LDA was performed using Origin software (OriginLab Corporation, USA) and was repeated on each hierarchical level for both the *in situ* full-resolution data and simulated multispectral data.

The discriminant analysis identified the variables that would maximize the differences among statistical species groups and minimize within-group differences. In stepwise discriminant analysis, at each step the program reviews all wavelengths and evaluates which one will contribute most to the discrimination between groups. Then, that wavelength will be included in the model and the program proceeds to the next step until all wavelengths are considered. The optimal sets of discriminant wavelengths are finally determined. To avoid overfitting and allow adequate discrimination, Wilk's lambda test statistic was used to show whether the discriminant functions significantly explained group membership. An α-level of 0.05 was chosen as the significance level to determine whether the corresponding variable should be included in the discriminant analysis. If the α-level values were smaller than 0.05, the values should be included in the discriminant analysis. Then, the

discriminant procedure was followed by calculating the separability accuracy between each group using the significant variables produced during the stepwise discriminant analysis. Moreover, to ensure the stability of the discriminant analysis classifiers, the cross-validation and variance of canonical variables for each group were used to show the separation accuracy. In the cross-validation, each training data point was treated as a test data point and excluded from the training data to judge which group it should be classified as; then, whether the classification was correct or not could be verified.

3.3 Discriminative abilities of the multispectral satellite sensors

The measured spectra were resampled to the multispectral bands of the Landsat 8 Operational Land Imager (OLI), Sentinel-2A, and World View-2 sensors. Multispectral sensors were selected because they are more widely available and more cost-effective remote sensing data sources than hyperspectral images. The Landsat 8 OLI has four water-penetrating bands. Sentinel-2A, with a 10-m spatial resolution, has three water-penetrating bands (bands 2, 3, and 4), and World View-2 has the highest number of water-penetrating bands from the coast to the red-edge (Figure 4). Sensors' reflectance spectra were simulated by applying the spectral response functions of three multispectral sensors to the *in situ* full-resolution spectra measurements. These simulated sensor spectra of the benthic objects comprise pure pixels without atmospheric or water column radiative transfer effects. Whereas the practical application of remote sensing for mapping requires atmospheric and water column corrections to derive the bottom reflected signal, errors and signal losses are inevitable in the correction process. Therefore, such a spectral separability analysis of simulated data is performed thus defining a theoretical upper limit on the discriminative abilities of the sensors.

4. Results

4.1 Spectral separability of typical substrate targets and species

4.1.1 Reflectance spectra characteristics of typical substrates

The averaged spectral reflectances and error bars of six typical substrates: *Enhalus acoroides* (*E. acoroides*), coral (*Siderastreidae*), white sand, the white attachment, dead coral debris, and bleached coral are shown in Figure 5. The white attachment is a certain kind of epiphytic algae, it has a wide distribution in our study area. Among them, white sand has the highest reflectance reaching 0.5–0.6, and its overall trend increases at 400–565 nm then decreases at 565–700 nm. The spectral characteristics of white sand obtained herein are different from those of sands measured in previous studies (Hochberg and Atkinson 2000; Karpouzli, Malthus, and Place 2004; Idris, Jean, and Zakariya 2009; Petit et al. 2017). White sand might be formed by the weathered accumulation of coral debris and might be lack of pigments, unlike general quartz sand. The high spectral similarity between white sand and coral debris might be related to the similarity of their compositions. The overall trend of the white attachment reflectance curve is the gentlest, slowly increasing and reaching a maximum at approximately 605 nm, then gradually decreasing, reaching the minimum near 670 nm, and exhibiting a sharp growth trend after 670 nm.

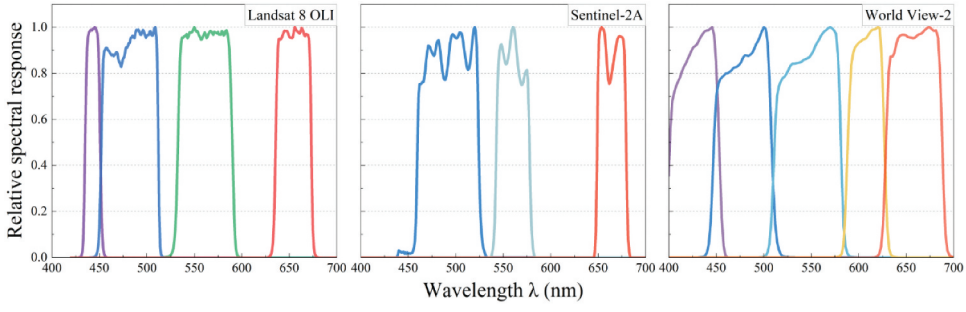

Figure 4. Relative spectral responses of the multispectral sensors: Landsat 8 OLI, Sentinel-2A, and World View-2.

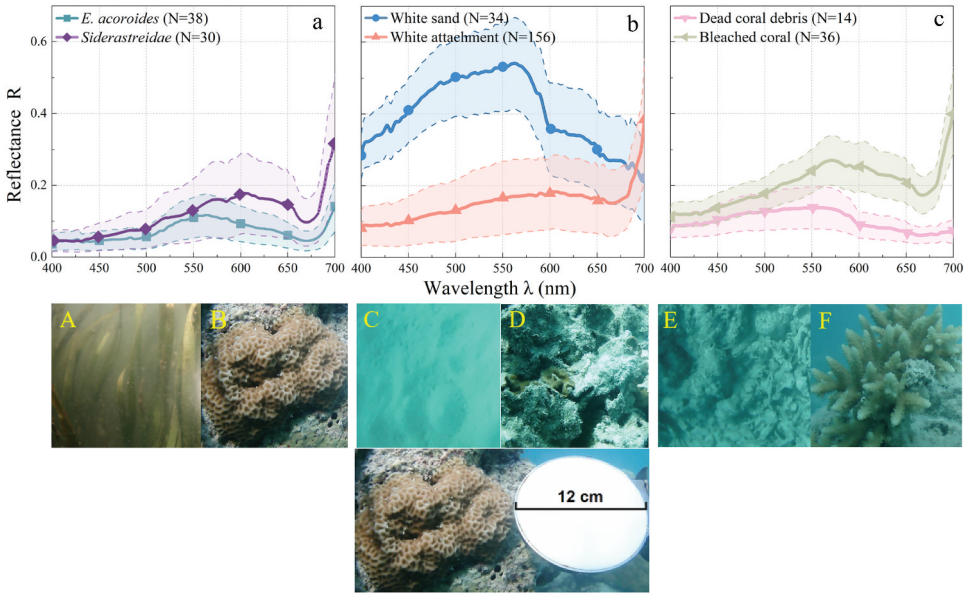

Figure 5. (a), (b), (c) Error bar graphs corresponding to the six substrate targets: *E. acoroides* (a), *Siderastreidae* (b), white sand (c), the white attachments (d), dead coral debris (e), and bleached coral (f). The solid line is the mean reflectance spectra for each substrate target, the error bars represent ±1 standard deviation as the square root of the pooled variances for each substrate, and N is the number of averaged spectra.

Coral (*Siderastreidae*), seagrass (*E. acoroides*), the white attachment, and partially bleached coral all have absorption peaks at approximately 670 nm and then rise sharply after 675 nm; this pattern is due to the presence of pigments (Karpouzli and Malthus 2003; Idris, Jean, and Zakariya 2009), such as chlorophyll a, chlorophyll c2, diatoxanthin, and β-carotene (Hedley and Mumby 2002; Hochberg et al. 2005). The overall reflectance curves of corals and seagrass have similar trends. Both show lower reflectances in the shorter wavelength region (400–500 nm), higher reflectances at 500–650 nm, characteristic absorption peaks at 670 nm, and steep rises at 675–700 nm. Nevertheless, coral and seagrass species exhibited differences in the magnitudes and overall shapes of their reflectances. The maximum coral reflectance value was measured at 605 nm, and a typical characteristic of corals is that they have obvious reflection characteristic peaks at approximately 570 nm and 605 nm and a shoulder peak at approximately 650 nm. In comparison, seagrass shows a reflectance maximum at nearly 565 nm and a broad peak at 500–650 nm. These spectral characteristics are consistent with those reported in previous studies (Holden and LeDrew 1998; Kutser et al. 2001; Yamano et al. 2002; Karpouzli and Malthus 2003).

The overall reflectance of partially bleached corals is higher than that of healthy corals, and the characteristic peaks of bleached corals at 605 nm and 650 nm are not obvious. Notably, partially bleached corals show the same characteristic peak at 570 nm as healthy corals and reach the maximum reflectance value around this wavelength. It seems that the characteristic peak of corals at 570 nm would not be influenced by the bleaching effect. The dead coral debris and white sand revealed differences in their reflectance magnitudes but were similar in their overall shapes. This result is consistent with the fact that both these substrates are composed of carbonates. The reflectance curves of both substrates show increases in the region of 400–565 nm, followed by decreases in the region of 565–650 nm. The dead coral debris, however, has a weak absorption peak near 670 nm and might be because of the residue of pigments or algae attachments. These results demonstrate that *in situ* reflectance data can accurately indicate and describe the material compositions and characteristics of different benthic substrates.

4.1.2 Discriminant classification of typical substrates

To quantitatively analyze the spectral separability of the typical substrates, we performed a classification analysis via LDA. Extended wavelengths from 390 to

700 nm were used in the stepwise discriminant analysis to extract further distinguishing information. Six typical substrate targets were discriminated was with eight noncontiguous wavelengths (400, 413, 500, 515, 568, 604, 623, and 645 nm) to set up the discriminant function using the *in situ* hyperspectral datasets. The established discriminant model includes five discriminant functions for the six typical substrate targets. In the scoring graph of the first two discriminant functions, the classes are unmistakably visible as distinct point clusters (Figure 6). White sand, seagrass (*E. acoroides*), and coral (*Siderastreidae*) are clearly separated from the other substrates, indicating their spectral distinctiveness.

The classification summary representing the training data table was used to evaluate the discriminant model (Table 2A). The mean *in situ* reflectance spectra discrimination accuracy of the six typical substrate targets was 97.5%. The classifications were 100% correct for the *E. acoroides*, dead coral debris, and *Siderastreidae* groups. The group with the highest classification error was bleached coral, which was misclassified as the white attachment with an error rate of 11.4%. We used the cross-validation method to ensure the stability of the discriminant analysis classifiers, and the cross-validation error rate of this model was 3.9%. Therefore, the discrimination of typical substrate targets was shown to be effective

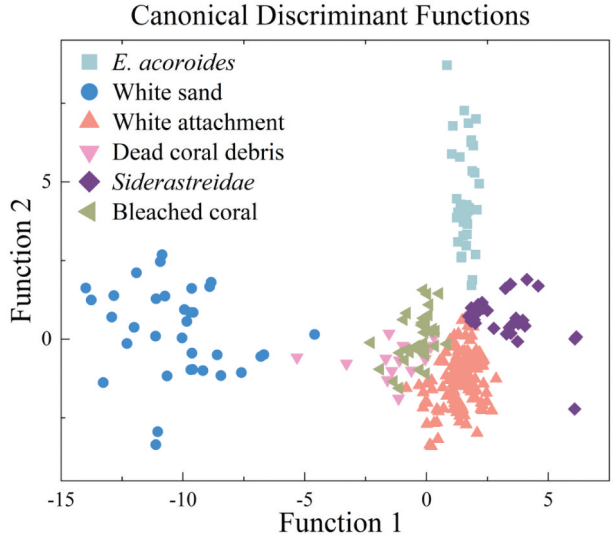

Figure 6. Scores from the LDA projected into the first two canonical discriminant function space that best separate the six typical substrate targets: *E. acoroides, Siderastreidae*, white sand, the white attachments, dead coral debris, and bleached coral.

using *in situ* hyperspectral reflectances. Compared with previous studies (Hochberg, Atkinson, and Andréfouët 2003; Karpouzli, Malthus, and Place 2004), the selected central discriminant wavelength had a relatively large correspondence, and the wavelength of 623 nm was also added to the discriminant model.

4.2 Spectral separability of different corals

4.2.1 Reflectance spectra characteristics of corals

We examined the spectral curves of different families (Figure 7(a)) and species (Figure 7(b)) of corals. The reflectance spectra of corals in the South China Sea commonly have the triple-peaked pattern described by Hochberg and Atkinson (2000) or the "brown" pattern (Hochberg, Atkinson, and Andréfouët 2003). Whereas differences in the reflectance magnitudes were observed, the spectral shapes of the reflectance features of all coral families were very similar (Figure 7(a)).

The low reflectance values at the blue and green wavelengths (400–525 nm), and the absorption peak at approximately 670 nm are primarily caused by the absorption of light by photosynthetic and photoprotective pigments (Enríquez, Méndez, and Prieto 2005; Niedzwiedzki et al. 2014). Higher values appear at 525–650 nm because of the lack of absorption and presence of active fluorescence at these wavelengths (Mazel 1995; Myers et al. 1999). In addition, the coral families have obvious positive reflectance characteristic peaks at approximately 570 nm and 605 nm and have either peaks or shoulder peaks near 650 nm. All coral reflectances have maximum values, generally 0.1–0.2, at 605 nm, while *Poritidae* shows a front peak near 570 nm. Exceptionally, the measurement depth of *Acroporidae* was approximately 5 m, which is deeper than those of the other families. The third reflection shoulder peak and the chlorophyll absorption peak of *Acroporidae* do not appear here due to the absorption and attenuation of the water column.

The *in situ* mean reflectance spectra of six *Acroporidae* species and underwater photographs of the corresponding species are shown in Figure 7(b). The spectra of all coral species exhibit overlapping absorption features. Disregarding the reflectance magnitude, most of the reflectances are similar, and most of the spectral peaks are consistent. Exceptionally, the trend is relatively flat in the 600–

Table 2. Classification rates for typical substrates, family-level, and species-level of corals using *in situ* reflectance spectra with the optimal wavelength set.

(A) Six typical substrate targets: cross-validation error rate = 3.9% (set of eight wavelengths: 400, 413, 500, 515, 568, 604, 623, and 645 nm)

	Predicted class						
	E. acoroides	White sand	White attachment	Dead coral debris	*Siderastreidae*	Bleached coral	Correct rate (%)
E. acoroides	**38**	0	0	0	0	0	100
White sand	0	**33**	0	1	0	0	97.1
White attachment	0	0	**155**	0	0	1	99.4
Dead coral debris	0	0	0	**14**	0	0	100
Siderastreidae	0	0	0	0	**30**	0	100
Bleached coral	0	0	4	0	0	**31**	88.6

(A) **(B) Nine families of corals: cross-validation error rate = 9.6% (set of 13 wavelengths: 395, 405, 418, 515, 528, 550, 575, 588, 640, 648, 659, 670, and 676 nm)**

	Predicted class									
	Acroporidae	*Agariciidae*	*Dendrophylliidae*	*Fungiidae*	*Lobophylliidae*	*Merulinidae*	*Pocilloporidae*	*Poritidae*	*Siderastreidae*	Correct rate (%)
Acroporidae	**187**	0	11	13	1	13	12	2	2	77.6
Agariciidae	0	**44**	2	5	0	0	0	1	0	84.6
Dendrophylliidae	0	0	**27**	0	0	0	0	0	0	100
Fungiidae	0	0	0	**32**	0	0	0	0	0	100
Lobophylliidae	0	0	0	0	**35**	0	0	0	0	100
Merulinidae	0	0	0	1	0	**25**	0	2	0	89.3
Pocilloporidae	0	0	2	0	0	0	**32**	2	0	88.9
Poritidae	0	0	6	2	0	0	2	**105**	0	91.3
Siderastreidae	0	0	4	0	0	0	0	0	**26**	86.7

(A) **(C) Six species of corals: cross-validation error rate = 9.8% (set of nine wavelengths: 401, 515, 521, 549, 576, 588, 640, 658, and 670 nm)**

	Predicted class						
	A. cerealis	*A. cytherea*	*A. hyacinthus*	*A. samoensis*	*A. humilis*	*A. austera*	Correct rate (%)
A. cerealis	**28**	5	0	0	1	0	82.4
A. cytherea	1	**90**	12	0	2	2	84.1
A. hyacinthus	1	6	**65**	0	3	3	83.3
A. samoensis	0	0	0	**31**	0	0	100
A. humilis	0	0	0	0	**14**	0	100
A. austera	0	0	0	0	0	**9**	100

Classification rates are the ratio of the number of predicted classes to the actual number of classes. Diagonal elements represent correct number of predicted classes, and off-diagonal elements represent misclassification number of predicted classes.

650 nm region of the reflectance curve of *Acropora sanoensis* (*A. samoensis*), which represents a "blue" pattern (Hochberg, Atkinson, and Andréfouët 2003). In addition, the *A. sanoensis* has the lowest reflectance values, with values generally less than 0.1.

4.2.2 Derivative spectral analysis of corals

Although the reflectance spectra curves of different corals are similar, the derivative spectra can amply show some nuances in the spectral responses expected from seemingly identical features. We compared the spectral shapes of each coral at the family level and species level by calculating the multiorder derivative of the reflectance. The derivative spectral analysis results are shown with a projection heat map Figure 8.

Obvious, relatively broad increases at 500–515 nm and negative region near 640 nm were observed in *Agariciidae, Lobophylliidae*, and *Siderastreida*. More obvious climbs than those seen in other families are found at 550–570 nm in *Acroporidae, Agariciidae*, and *Lobophylliidae* (Figure 8(a,b)). The first derivative spectra of *Acroporidae, Fungiidae, Merulinidae*, and *Poritidae* showed positive values at 650–655 nm, while other corals were not recognizable. Furthermore, *Dendrophylliidae* presented significant differences between 465–475 nm and 605–615 nm compared to the other families (Figure 8(b–d)) and showed more distinct dips at 460–470 and 518–523 nm. The comparison of the second derivative spectra shows that the reflectance spectra curves of most of the studied corals have slight bulges at 670–675 nm, while this trend is relatively insignificant for *Agariciidae, Merulinidae*, and *Siderastreidae* (Figure 8(b,f)).

Among the species of *Acroporidae*, the first derivative spectra of *A. sanoensis* reveals decreasing trends at approximately 485 nm and 520 nm and a slight

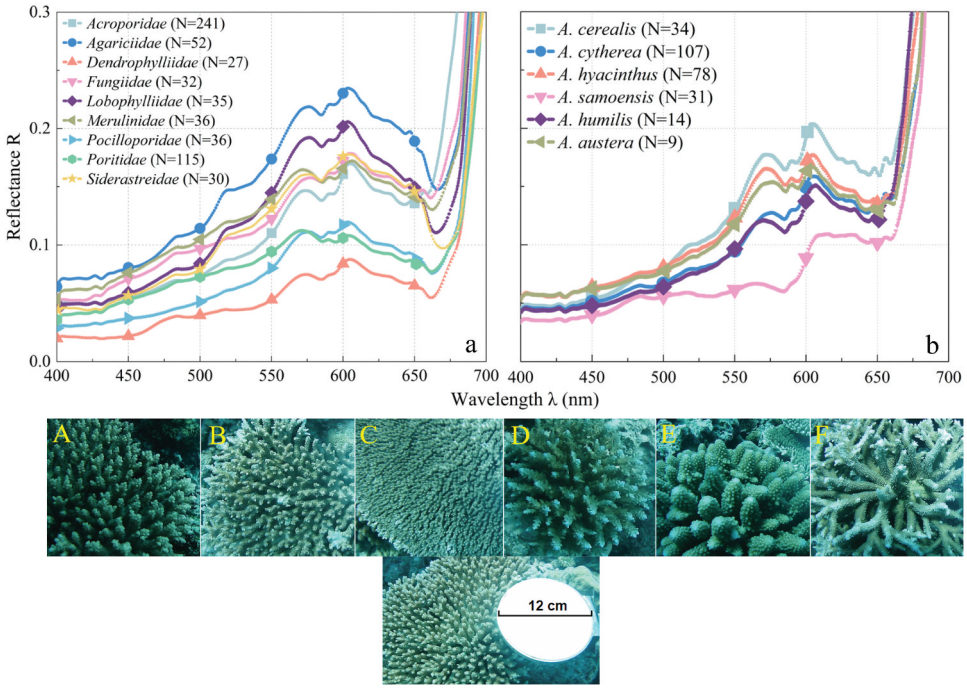

Figure 7. (a) *In situ* mean reflectance spectra of nine families of coral: *Acroporidae, Agariciidae, Dendrophylliidae, Fungiidae, Lobophylliidae, Merulinidae, Pocilloporidae, Poritidae*, and *Siderastreidae*. (b) *In situ* averaged reflectance spectra of six species of *Acroporidae: A. cerealis* (a), *A. cytherea* (b), *A. hyacinthus* (c), *A. sanoensis* (d), *A. humilis* (e), and *A. austere* (f). N is the number of averaged spectra.

decrease at 610–630 nm; this pattern is distinct from those of other species (Figure 8(e)). Notably, *Acropora humilis* (*A. humilis*) and *Acropora hyacinthus* (*A. hyacinthus*) have uncharacteristic features characterized by positive increases at approximately 658 nm. The third derivative shows that *A. humilis* has a specific negative characteristic near 678 nm and a negative value similar to that of *Acropora austere* (*A. austere*) at approximately 625 nm (Figure 8(g)). Furthermore, *Acropora cerealis* (*A. cerealis*) has a distinct third derivative signature that discriminates it from the other corals, displaying opposite values near 614 and 676 nm. Nearly all peaks in the derivative spectra occur within narrow wavelength ranges, sometimes as broad as 20 nm, but often on the order of 10 nm. Previous studies have utilized derivative spectroscopy to distinguish different substrates such as sand, seagrass, seaweed, and coral (Hochberg and Atkinson 2000; Minghelli-Roman et al. 2002; Hwang et al. 2019), as well as different health states of corals (Holden and LeDrew 1998; Yamano et al. 2002, 2003). All these studies indicate that derivative spectroscopy could effectively enhance spectral differences. Our results reveal that the spectrum differences of corals almost focused on the wavelengths ranged from 550 to 680 nm. Most of the multiorder derivative differences, however, are in the narrow bands (<10 nm) and these differences may not robust among the different coral species and environments. Therefore, the differences of derivative spectral reported here should be interpreted with caution.

4.2.3 Discriminant classification of corals

From the classification summary of the training data table, the overall discrimination accuracies of the *in situ* reflectance spectra of nine families and six species of coral were 90.9% (Table 2B) and 91.6% (Table 2C), respectively. Family-level discrimination was achieved using stepwise discriminant analysis to determine the optimal wavelengths with 13 non-contiguous wavelengths (395, 405, 418, 515, 528, 550, 575, 588, 640, 648, 659, 670, and 676 nm). Similarly, nine wavelengths (401, 515, 521, 549, 576, 588, 640, 658, and 670 nm) were selected for discrimination at the species-level. Accordingly, several wavelengths were common among each discriminant level, and a set of wavebands centered on 403, 515, 525, 550, 576, 588, 640, 659, and 670 nm could be seen as suitable for the classification at corals. In a comparison of the wavelength subsets identified

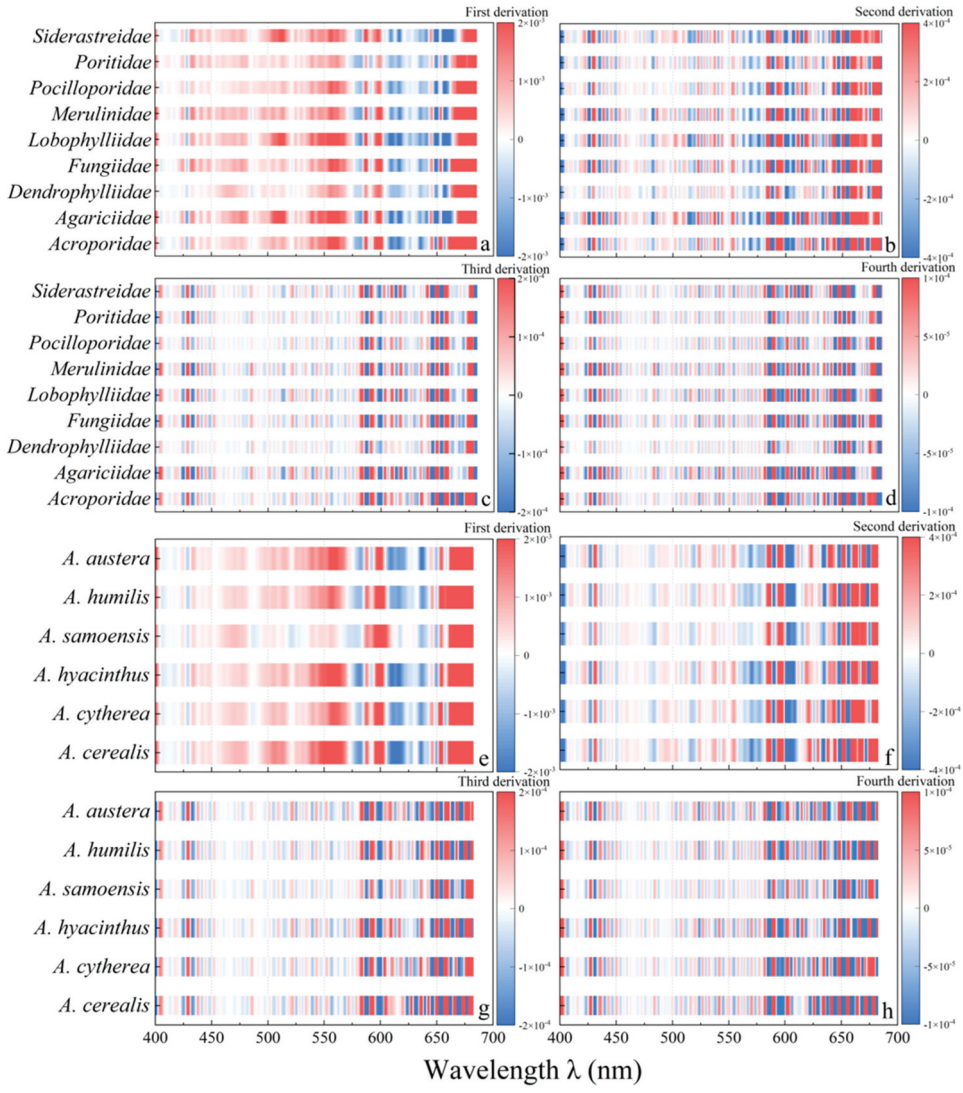

Figure 8. Projection heat maps of the first (a, e), second (b, f), third (c, g), and fourth (d, h) derivative spectra of nine families of corals (a, b, c, d): *Acroporidae, Agariciidae, Dendrophylliidae, Fungiidae, Lobophylliidae, Merulinidae, Pocilloporidae, Poritidae*, and *Siderastreidae*. In addition, six species of *Acroporidae* (e, f, g, h): *A. austere, A. humilis, A. sanoensis, A. hyacinthus, A. cytherea*, and *A. cerealis*. The red, blue, and white colors represent the positive, negative, and zero values of the derivative spectra, respectively, and the color shades represent the value magnitudes.

via LDA method in this study with those determined in previous research (Hochberg, Atkinson, and Andréfouët 2003; Karpouzli, Malthus, and Place 2004), these wavelengths agree closely with several previously reported wavebands centered at 405, 418, 528, 576, 640, and 670 nm.

The classification accuracy was 100% correct for the families groups of *Dendrophylliidae, Fungiidae*, and *Lobophylliidae* and the species of *A. samoensis, A. humilis*, and *A. austere*. The class with the highest classification error was *Acroporidae*, which tended to be one-way misclassified as several families with error rates of approximately 5%, including *Dendrophylliidae, Fungiidae, Merulinidae*, and *Pocilloporidae*. Furthermore, at the species level, *A. cerealis* had the highest classification error and tended to be one-way misclassified as *Acropora cytherea* (*A. cytherea*) with an error rate of 14.7%. To ensure the stability of the discriminant analysis classifiers, we used the cross-validation method to perform the model validation, and the cross-validation error rates of the two models are 9.6% and 9.8%, respectively. Consequently, the use of *in situ* hyperspectral reflectance datasets to identify species differences between and within taxonomic coral groups was shown to be effective.

Eight discriminant functions were created for the family level, and five discriminant functions were created for the species level via canonical discriminant analysis to construct a discriminant model. In the scoring graph of the first two discriminant functions, these classes are undoubtedly visible as distinct point clusters (Figure 9). The most distinct cluster among *Acroporidae* was the species of *A. samoensis*. The examination of the LDA results indicated that the spectral separation of various corals was more apparent at the species level than at the family level. Although this may seem to contradict previous studies in which the classification accuracy decreased with increasing descriptive resolution levels, only *Acroporidae* had an evident prediction accuracy in this study. This is because *Acroporidae* has the highest species diversity and the most significant number of members in the available datasets, such that the reflectance spectra of *Acroporidae* have a wider distribution range which contains the variability of diverse coral species. Then this variability will lead to confusion in the classification results.

4.3 Discriminative abilities of the multispectral satellite sensors

Figure 10 shows the mean reflectance spectra for each substrate target, revealing the sensor spectra from three classification levels. White sand is the brightest among the six typical substrates (Figure 10(a,d,g)). *Acroporidae* and *Fungiidae* have unique features in that their overall spectral curves show increasing trends (Figure 10(b,e,h)). This is because the *in situ* measurement depths of both families are located at approximately 5 m, which is deeper than those of the other families, and no chlorophyll absorption peak appears in these spectra because of the effects of the water column. Furthermore, in the World View-2 spectra, *A. humilis* decreases near the 610–660 nm waveband, which is different from other species of *Acroporidae* (Figure 10(i)). Various species of *Acroporidae*, however, appear virtually identical in the Landsat 8 OLI and Sentinel-2A spectra.

The discriminant analyses were repeated on spectra treated with the spectral response functions of the multispectral sensors to investigate the spectral limitations of the multispectral satellite sensors. The LDA scores revealing the sensor spectra that best separated the substrate targets are shown in Figure 11. All the sensors offered identical canonical discriminant function distributions at the typical substrate level, providing nearly equivalent spectral separations (Figure 11(a,d,g)). White sand is visible as a very distinct point cluster in all sensor spectra. This appearance shows that the spectral separation of white sand is apparent via an examination of the LDA results. Despite some overlap among the six typical substrates, their separation still appears. The LDA results for different corals among the multispectral sensors, however, have a greater overlap than the full-resolution results, regardless of the family or species level. Exceptionally, *A. samoensis*, which exhibited a "blue" pattern, still showed distinct cluster points (Figure 11(c,f,i)). Therefore, these multispectral sensors may not provide adequate spectral separation of different families or species of corals.

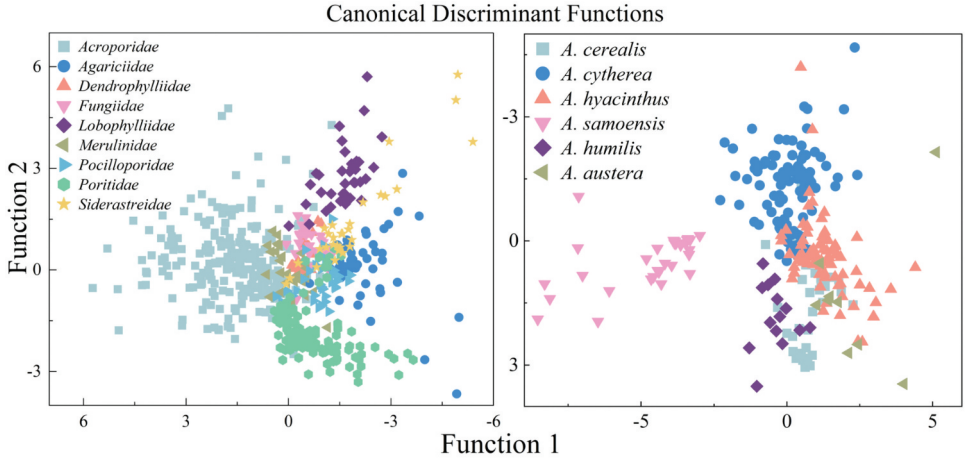

Figure 9. Scores from the discriminant function analysis projected into the first two canonical discriminant function space of the first two functions that best separate the coral substrates. (a) Family-level classes; (b) species-level classes. Missing letter numbers

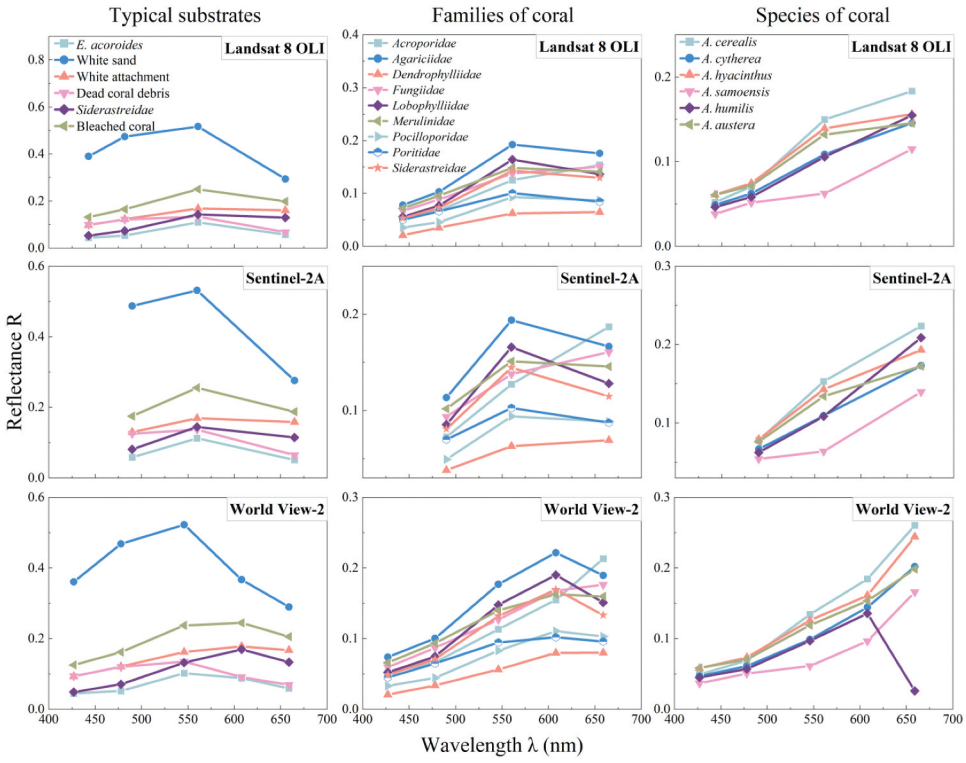

Figure 10. Spectral signatures in each spectral band for six typical substrates (a, d, g), nine families of corals (b, e, h), and six species of *Acroporidae* (c, f, i) as shown in the sensor spectra. Four bands of Landsat 8 OLI, three bands of Sentinel-2A, and five bands of WorldView-2 were used, with only visible bands included in the resampling process. Missing letter numbers

These spectral separations, however, may be apparent via the examination of the LDA results for the different typical substrates and spectral patterns of corals with visual spectral differences.

The results of the classification summary of the simulated sensor spectra are shown in Figure 12 and Table 3. The discriminant analysis of the six typical substrates indicates their spectral separability, with overall discrimination accuracies of 89.6%, 88.2%, and 90.4% for the Landsat 8 OLI, Sentinel-2A, and World View-2 sensors, respectively (Figure 12(a,d,g)). Bleached coral had the lowest accuracy rate for all sensors and primarily tended to be misclassified as the white attachment, with error rates of 20.0%, 22.9%, and 22.9%. Although the error rate is very small at less than 8%, a two-way misclassification existed between dead coral debris and white sand in the Landsat 8 OLI and Sentinel-2A sensor spectra. World View-2 provided a 100% accuracy in identifying dead coral debris. In addition, all sensors show that both seagrass (*E. acoroides*) and coral (*Siderastreidae*) have similar but weak trends to be misclassified as the white attachment, with a maximal error rate of 16.7%.

The overall discrimination accuracies of the nine families and six species of corals were 67.1% and 70.0%, respectively, for the Landsat 8 OLI (Figure 12(b, c)), 56.0% and 56.0% for the Sentinel-2A sensor (Figure 12(e,f)), and 64.5% and 61.8% for the World View-2 sensor (Figure 12(h,i)). *Agariciidae* has the lowest accuracy rates of 7.7%, 9.6%, 13.5% for the Landsat 8 OLI, Sentinel-2A, and World View-2 sensors, respectively (Figure 12(b,e,h)). Except for *Dendrophylliidae, Fungiidae*, and *A. samoensis*, all sensors exhibited considerable confusion among different corals regardless of the family or species level. Although *Dendrophylliidae* and *Fungiidae* had almost 100% discriminant accuracies in all sensors, several families were misclassified as *Dendrophylliidae* by the Sentinel-2A sensor, such as *Acroporidae, Pocilloporidae, Poritidae*, and *Siderastreidae*.

5. Discussion

Mapping benthic objects using remote sensing images relies on a particular object presenting a spectrally distinguishable reflectance (Karpouzli and Malthus 2003; Kutser, Dekker, and Skirving

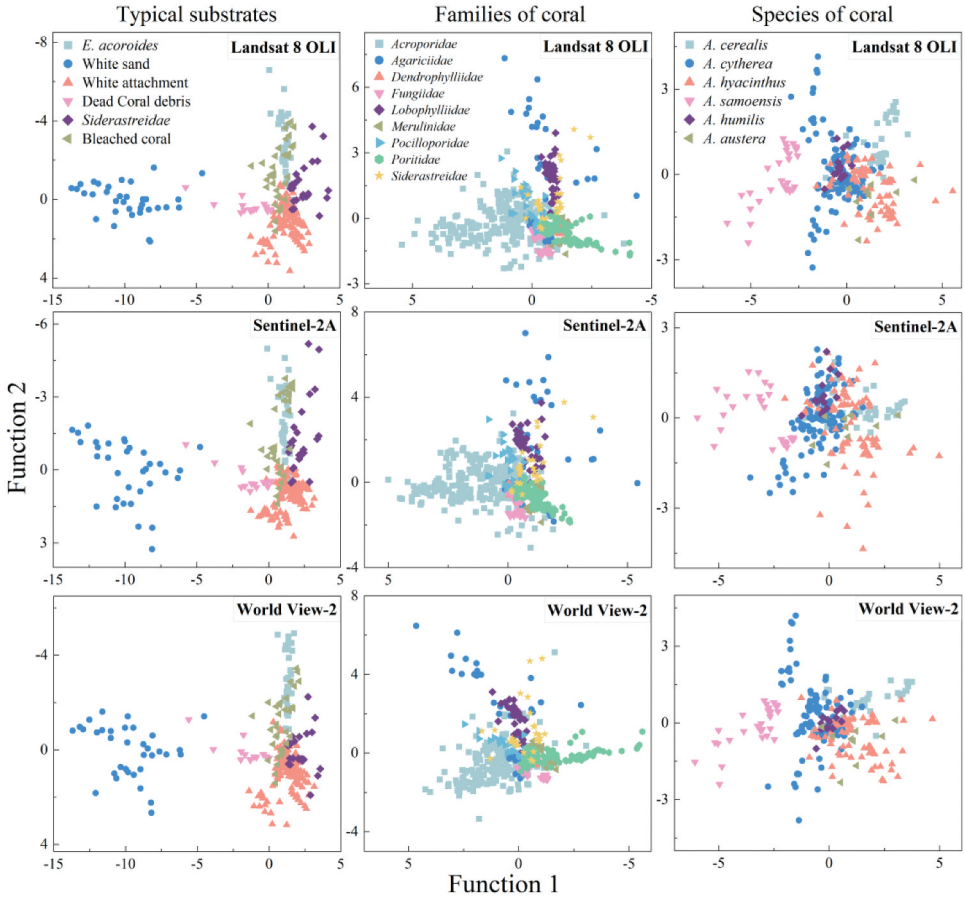

Figure 11. Scores from the LDA for sensor spectra projected into the first two canonical discriminant function space that best separate the substrate targets in multiple classification levels. This analysis included six typical substrates (a, d, g), nine families of coral (b, e, h), and six species of *Acroporidae* (c, f, i). Missing letter numbers

2003). However, there is no reported standard for measuring sea-bottom reflectance and no widely used commercial instrument since the substrates are in complex light field environments. Except that some underwater measurement platforms were built specifically for certain studies (Hochberg and Atkinson 2000; Kutser, Dekker, and Skirving 2003; Roelfsema and Phinn 2012). A set of reflectance-measuring instruments suitable for aquatic marine environments were specifically designed to obtain the *in situ* reflectance spectra of various substrate targets. The instruments were double-calibrated under the standard optical conditions of the laboratory and the underwater environment. Furthermore, the reflectance measurements fully considered and optimized the spectral resolution, absorption, and attenuation of the water column as well as the complexity of the underwater light field. Therefore, the measurements exactly represented the *in situ* reflectance spectra of the substrate targets.

Although the number of spectra analyzed in this paper is less than that obtained in a previous worldwide study (Hochberg and Atkinson 2003), the measurement methods utilized herein have taken full account of the error factors in underwater measurements. In addition, no relevant reflectance dataset has previously been established in the South China Sea. The spectral separability findings obtained in this study demonstrated that it is possible to perform spectral discrimination of coral reef communities from multiple classification levels using *in situ* hyperspectral reflectance data under the conditions of pure endmember, perfect atmospheric and water column correction. Each substrate has characteristic features that enable its identification or discrimination, the fundamental requirement for coral reef remote sensing. Effective monitoring, however, requires significant substratum features to be detectable by a sensor (Botha et al. 2013). Furthermore, submerged benthic community mapping using remote sensing

techniques is limited to the visible bands due to strong energy attenuation by the water column. The capability of mapping coral species using multispectral images appears to be constrained by the nature of the spectral variation and the inadequacy of the spectral resolution. Spectral separations may be apparent for typical substrates with distinctive spectral patterns as pure endmembers, even when using multispectral sensors. Hochberg and Atkinson (2003) evaluated the classification abilities of several airborne hyperspectral and satellite multispectral sensors and two designed hypothetical sensors for the discrimination of coral, algae, and carbonate sand. Their studies revealed the potential design of a narrowband multispectral sensor with appropriate wavebands for assessing coral reef status. However, the spectra of substrate targets frequently overlap. These spectra are not always separable in optical remote sensing images due to the small numbers of broad bands (Wicaksono et al. 2019), particularly when there is water column interference as a result of coral reef communities being submerged during the satellite sensor overpass.

5.1 Bottom reflectance detectability in the water column

Previous studies have revealed that the geographic location has no effect on the spectral characteristics of coral reef features (Holden and LeDrew 1999; Hochberg, Atkinson, and Andréfouët 2003). Measurements of the same substrate across biogeographic regions are spectrally consistent. The bottom-reflectance feature, however, is not always directly observable because the effects of absorption and scattering change the radiant fluxes in the overlying water column. For substrates located at different water depths and/or different water properties, these conditions modify some reflectance features. Moreover, different wavelengths of light are attenuated to varying degrees by the water column.

The optical detectability of substrates in coral reefs can be characterized by the attenuation coefficient and the light penetration depth. The diffuse attenuation coefficient, K_d, can be estimated from *in situ* measurements of the vertical profile of the downwelling irradiance, E_d, as the linear regression slope in a plot of $\ln(E_d)$ versus z over the depth range of interest. The characterization of light penetration shown in Figure 13 is an average of 30 individual representative stations, and the 95% confidence intervals were calculated based on a t-distribution with the number of samples, n, set to 30. The light attenuation first decreases to reach a minimum at 485 nm and then increases with the wavelength. The light in the red region has low penetration, and for this reason, when mapping deeply submerged substrates using remote sensing techniques, only the blue and green regions are useful. The effective penetration depth was calculated from the diffuse attenuation coefficient along the water column, expressed in the model as z_{90} (Figure 13(b)), which is the layer thickness from which 90% of the total radiance originates (Zoffoli, Frouin, and Kampel 2014; Gordon and McCluney 1975). The results reveal that the maximum bottom detectability depth was less than 10 m at wavelengths greater than 600 nm under the optical scenario of a clear-water coral reef.

5.2 Responses of reflectance spectra at different water depths

Although *in situ* hyperspectral reflectance data can be used to identify different coral species, the depth of the corals that can be used to detect selected optimal discriminant wavelength signals in the water surface may be less than 4 m. For rough substrate classification levels, such as differentiations among corals, seagrasses, sands, and other sediments, the maximum substrate identification depth is within 5–10 m and depends on the turbidity of the water and substrate types.

The reflectance spectra of the same substrate target at different water depths and matching photographs are shown in Figure 14. In deeper water, the reflected red band signal of the same target gradually disappears, and the "steeply rising" reflectance band moves anteriorly. However, the reflectance characteristics of the blue-green band are unaffected. Therefore, as long as light can reach the bottom, the variation in the surrounding environment does not affect the reflectance characteristics of the substrate target. Furthermore, the consistency between the spectral reflectance responses at different depths and the light penetration also demonstrates that it is reliable to measure the sea-bottom reflectance under variable underwater environments.

The spectral signature of a coral species is limited and determined by its genetic makeup and symbionts (Niedzwiedzki et al. 2014; Torres-Perez et al. 2015).

Table 3. Classification rates for typical substrates, family-level, and species-level of corals using *simulated* reflectance spectra.

Satellite sensors	(A) Six typical substrate targets					
	E. acoroides (%)	White sand (%)	White attachment (%)	Dead coral debris (%)	*Siderastreidae* (%)	Bleached coral (%)
Landsat 8 OLI	89.5	97.1	97.4	92.9	86.7	74.3
Sentinel-2A	94.7	97.1	99.4	92.9	76.7	68.6
World View-2	86.8	97.1	96.8	100	90.0	71.4

	(B) Nine families of corals								
	Acroporidae (%)	*Agariciidae (%)*	*Dendrophylliidae (%)*	*Fungiidae (%)*	*Lobophylliidae* (%)	*Merulinidae* (%)	*Pocilloporidae* (%)	*Poritidae* (%)	*Siderastreidae* (%)
Landsat 8 OLI	55.2	7.7	100	96.9	77.1	82.1	88.9	52.2	43.3
Sentinel-2A	58.9	9.6	96.3	90.6	71.4	67.9	38.9	43.5	26.7
World View-2	49.4	13.5	100	100	68.6	82.1	75.0	58.3	33.3

	(C) Six species of corals					
	A. cerealis (%)	*A. cytherea (%)*	*A. hyacinthus (%)*	*A. samoensis*(%)	*A. humilis* (%)	*A. austera* (%)
Landsat 8 OLI	76.5	45.8	46.2	100	71.4	77.8
Sentinel-2A	76.5	44.9	18.0	80.7	71.4	44.4
World View-2	76.5	59.8	46.2	100	21.4	66.7

Classification rates are the ratio of the number of predicted classes to the actual number of classes.

However, both the naturally occurring variations within a species and changes in environmental conditions modify the expressed spectral signatures of corals. Substrates that are located at different depths or exposed to different light field environments present wider spectral variation, increasing the spectral variability within benthic species. Further spectral research work is also necessary to enrich the spectral database of coral reefs. Theoretically, such a spectral library can characterize all substrate characteristic and water property combinations, and then the spectral matching method can be used to retrieve information

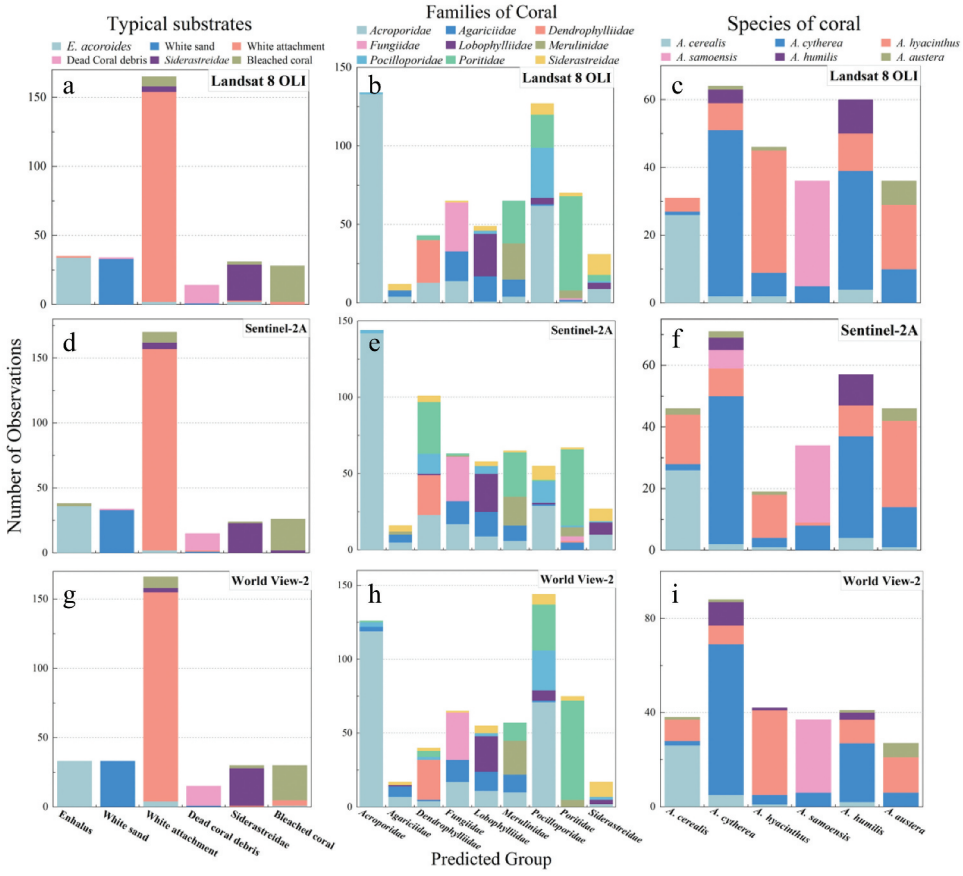

Figure 12. Classification summary plots of the six typical substrates (a, d, g), nine families of coral (b, e, h), and six species of *Acroporidae* (c, f, i) were obtained with the simulated sensor spectra.

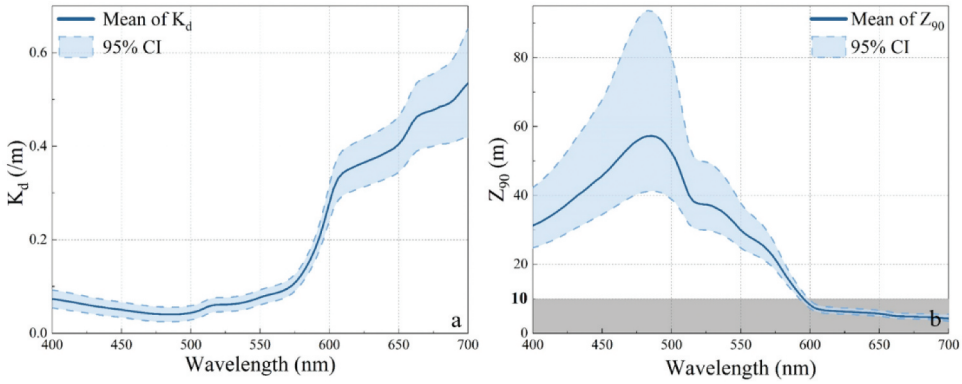

Figure 13. Light decay modeled along the water column, expressed as K_d and z_{90} as functions of the wavelength. (a) Average diffuse attenuation coefficient measured in the Xisha Islands coral reef areas; (b) the spectral depth of the penetration of light, z_{90}, calculated from the diffuse attenuation coefficient. The solid line is the mean data, and the shaded part is the 95% confidence interval (CI) of the measurements.

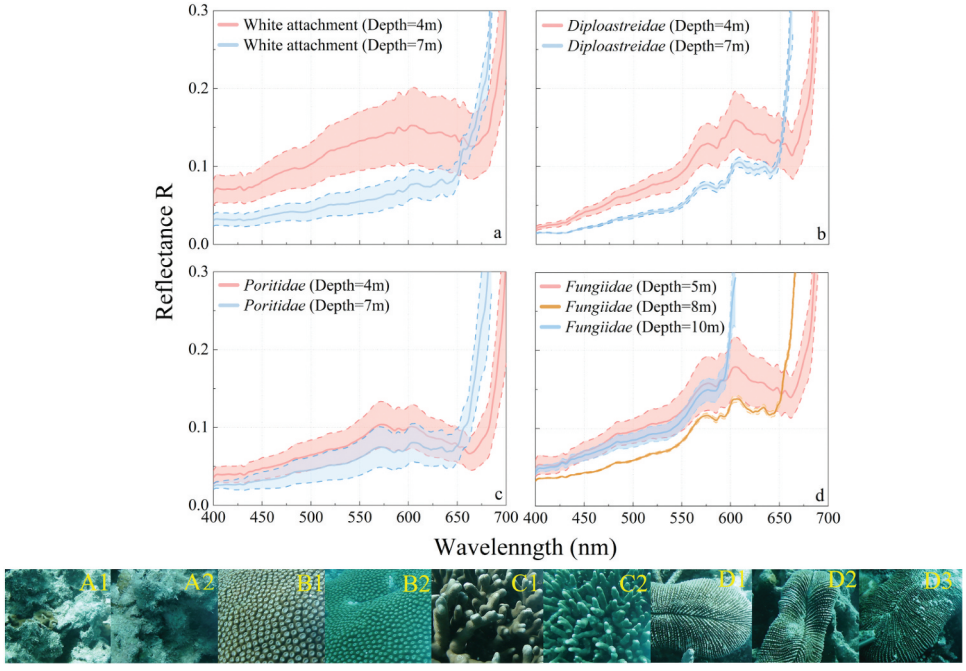

Figure 14. Reflectance spectra of the same substrate target at different water depths. (a) The white attachment at 4 m (A1) and 7 m (A2); (b) *Diploastreidae* at 4 m (B1) and 7 m (B2); (c) *Poritidae* at 4 m (C1) and 7 m (B2); and (d) *Fungiidae* at 5 m (D1), 8 m (D2), and 10 m (D3). The solid line is the mean reflectance spectra of corresponding substrate, and the error bars represent ±1 standard deviation as the square root of the pooled variances for each substrate.

(Mobley et al. 2005; Kutser, Miller, and Jupp 2006; Lesser and Mobley 2007). Therefore, in the future, establishing a comprehensive and continually optimized spectral library requires the integration of global substrate reflectance data and necessitates unified measurement specifications and data standards.

6. Conclusion

In this work, a hyperspectral sea-bottom reflectance measuring instrument that is suitable for accurate radiation measurements in complex shallow water environments such as coral reefs was specifically

designed to observe the optical properties of benthic communities. Based on *in situ* hyperspectral reflectance data, the reflectance spectral characteristics of various substrate targets were clarified and discriminated. The use of derivative spectroscopy amplified the spectral differences among and within taxonomic groups to distinguish different corals. The reflectance spectra between corals exhibited certain differences in the 550–680 nm. This finding suggested that the wavelengths of 550–680 nm have the potential to allow discriminations among different corals.

We conclude that there is a potential to classify various substrate targets in communities and taxonomic coral groups using *in situ* hyperspectral reflectance data. Furthermore, multispectral sensors are currently inadequate for spectrally separate corals. Nevertheless, spectral separations may be possible for different substrate targets with visual spectral differences. Our results serve as general guidelines for detecting benthic species living in coral reefs using remote sensors. The sea-bottom reflectance measuring instrument designed herein represents a promising means with which to examine the feasibility of remote sensing applications for the mapping and ecological monitoring of coral reefs in general.

Acknowledgements

We are grateful to Sumin Liu, Zifeng Cai, and Ziwei Yao for their field assistance at Sanya and Xisha Islands. We also express our appreciation to colleagues in the Optics Laboratory at the South China Sea Institute of Oceanology, Chinese Academy of Sciences, who contributed to designing and developing the sea-bottom reflectance measuring instrument used in this study.

Disclosure statement

No potential conflict of interest was reported by the author(s).

Funding

This work was supported by the National Natural Science Foundation of China (NSFC) (42076190, 41776044); the Key Special Project for Introduced Talents Team of Southern Marine Science and Engineering Guangdong Laboratory (Guangzhou) (GML2019ZD0305); the Key Deployment Project of Centre for Ocean Mega-Research of Science, Chinese Academy of Science (COMS2019J10); the Basic and applied basic Research Foundation of Guangdong Province (2021A1515011538); the Special Project for Marine Economic Development (Six Major Marine Industries) of Guangdong Province (GDNRC2020019); and the Key Research and Development Program of Hainan Province (ZDYF2021XDNY131).

Data availability statement

The data that support the findings of this study are available from the corresponding author, Z. X., upon reasonable request. Data private access link: https://www.scidb.cn/en/s/Ib6fAj

References

Ackleson, S. G. 2003. "Light in Shallow Waters: A Brief Research Review." *Limnology and Oceanography* 48 (1): 323–328. doi:10.4319/lo.2003.48.1_part_2.0323.

Barnes, B. B., C. Hu, B. A. Schaeffer, Z. Lee, D. A. Palandro, and J. C. Lehrter. 2013. "MODIS-derived Spatiotemporal Water Clarity Patterns in Optically Shallow Florida Keys Waters: A New Approach to Remove Bottom Contamination." *Remote Sensing of Environment* 134: 377–391. doi:10.1016/j.rse.2013.03.016.

Botha, E. J., V. E. Brando, J. M. Anstee, A. G. Dekker, and S. Sagar. 2013. "Increased Spectral Resolution Enhances Coral Detection under Varying Water Conditions." *Remote Sensing of Environment* 131: 247–261. doi:10.1016/j.rse.2012.12.021.

Caras, T., and A. Karnieli. 2013. "Ground-level Spectroscopy Analyses and Classification of Coral Reefs Using a Hyperspectral Camera." *Coral Reefs* 32 (3): 825–834. doi:10.1007/s00338-013-1033-1.

Chen, B. Q., Y. M. Yang, D. W. Xu, and E. H. Huang. 2019. "A Dual Band Algorithm for Shallow Water Depth Retrieval from High Spatial Resolution Imagery with No Ground Truth." *Isprs Journal of Photogrammetry and Remote Sensing* 151: 1–13. doi:10.1016/j.isprsjprs.2019.02.012.

Demetriades-Shah, T. H., M. D. Steven, and J. A. Clark. 1990. "High Resolution Derivative Spectra in Remote Sensing." *Remote Sensing of Environment* 33 (1): 55–64. doi:10.1016/0034-4257(90)90055-Q.

Enríquez, S., E. R. Méndez, and R. I. Prieto. 2005. "Multiple Scattering on Coral Skeletons Enhances Light Absorption by Symbiotic Algae." *Limnology and Oceanography* 50 (4): 1025–1032. doi:10.4319/lo.2005.50.4.1025.

Gapper, J. J., H. El-Askary, E. Linstead, and T. Piechota. 2018. "Evaluation of Spatial Generalization Characteristics of a Robust Classifier as Applied to Coral Reef Habitats in Remote Islands of the Pacific Ocean." *Remote Sensing* 10 (11): 21. doi:10.3390/rs10111774.

Garcia, R., Z. Lee, and E. Hochberg. 2018. "Hyperspectral Shallow-Water Remote Sensing with an Enhanced Benthic Classifier."*Remote Sensing* 10 (1): 25. doi:10.3390/rs10010147

Gege, P. 2004. "The Water Color Simulator WASI: An Integrating Software Tool for Analysis and Simulation of Optical in Situ Spectra." *Computers & Geosciences* 30 (5): 523–532. doi:10.1016/j.cageo.2004.03.005.

Gege, P. 2014. "WASI-2D: A Software Tool for Regionally Optimized Analysis of Imaging Spectrometer Data from Deep and Shallow Waters." *Computers & Geosciences* 62: 208–215. doi:10.1016/j.cageo.2013.07.022.

Gordon, H. R., and W. R. McCluney. 1975. "Estimation of the Depth of Sunlight Penetration in the Sea for Remote Sensing." *Applied Optics* 14 (2): 413–416. doi:10.1364/AO.14.000413.

Hardy, J. T., F. E. Hoge, J. K. Yungel, and R. E. Dodge. 1992. "Remote Detection of Coral 'Bleaching' Using Pulsed-laser Fluorescence Spectroscopy." *Marine Ecology Progress Series* 88 (2–3): 247–255. doi:10.3354/meps088247.

Hedley, J., B. Russell, K. Randolph, and H. Dierssen. 2016. "A Physics-based Method for the Remote Sensing of Seagrasses." *Remote Sensing of Environment* 174: 134–147. doi:10.1016/j.rse.2015.12.001.

Hedley, J. D., and P. J. Mumby. 2002. "Biological and Remote Sensing Perspectives of Pigmentation in Coral Reef Organisms." *Advances in Marine Biology* 43: 277–317. doi:10.1016/s0065-2881(02)43006-4.

Hedley, J. D., P. J. Mumby, K. E. Joyce, and S. R. Phinn. 2004. "Spectral Unmixing of Coral Reef Benthos under Ideal Conditions." *Coral Reefs* 23 (1): 60–73. doi:10.1007/s00338-003-0354-x.

Hedley, J., C. Roelfsema, B. Koetz, and S. Phinn. 2012. "Capability of the Sentinel 2 Mission for Tropical Coral Reef Mapping and Coral Bleaching Detection." *Remote Sensing of Environment* 120: 145–155. doi:10.1016/j.rse.2011.06.028.

Hochberg, E. J., and M. J. Atkinson. 2000. "Spectral Discrimination of Coral Reef Benthic Communities." *Coral Reefs* 19 (2): 164–171. doi:10.1007/s003380000087.

Hochberg, E. J., A. Apprill, M. J. Atkinson, and R. R. Bidigare. 2005. "Bio-optical Modeling of Photosynthetic Pigments in Corals." *Coral Reefs* 25 (1): 99–109. doi:10.1007/s00338-005-0071-8.

Hochberg, E. J., and M. J. Atkinson. 2003. "Capabilities of Remote Sensors to Classify Coral, Algae, and Sand as Pure and Mixed Spectra." *Remote Sensing of Environment* 85 (2): 174–189. doi:10.1016/S0034-4257(02)00202-X.

Hochberg, E. J., M. J. Atkinson, and S. Andréfouët. 2003. "Spectral Reflectance of Coral Reef Bottom-types Worldwide and Implications for Coral Reef Remote Sensing." *Remote Sensing of Environment* 85 (2): 159–173. doi:10.1016/S0034-4257(02)00201-8.

Hochberg, E. J., M. J. Atkinson, A. Apprill, and S. Andrfout. 2004. "Spectral Reflectance of Coral." *Coral Reefs* 23 (1): 84–95. doi:10.1007/s00338-003-0350-1.

Holden, H., and E. LeDrew. 1997. Spectral identification of coral biological vigour, Igarss '97-1997 International Geoscience and Remote Sensing Symposium, Proceedings Vols I-Iv: Remote Sensing - a Scientific Vision for Sustainable Development, New York: I E E E.

Holden, H., and E. LeDrew. 1998. "Spectral Discrimination of Healthy and Non-healthy Corals Based on Cluster Analysis, Principal Components Analysis, and Derivative Spectroscopy." *Remote Sensing of Environment* 65 (2): 217–224. doi:10.1016/S0034-4257(98)00029-7.

Holden, H., and E. LeDrew. 1999. "Hyperspectral Identification of Coral Reef Features." *International Journal of Remote Sensing* 20 (13): 2545–2563. doi:10.1080/014311699211921.

Huang, H., Z. Dong, and J. Lian. 2008. "Establishment of Nature Reserve of Coral Reef Ecosystem on the Xisha Islands." *Tropical Geography* 28 (6): 540–544.

Huguenin, R. L., and J. L. Jones. 1986. "Intelligent Information Extraction from Reflectance Spectra: Absorption Band Positions." *Journal of Geophysical Research: Solid Earth* 91 (B9): 9585–9598. doi:10.1029/JB091iB09p09585.

Hwang, C., C. H. Chang, M. Burch, M. Fernandes, and T. Kildea. 2019. "Spectral Deconvolution for Dimension Reduction and Differentiation of Seagrasses: Case Study of Gulf St. Vincent, South Australia." *Sustainability* 11 (13): 3695. doi:10.3390/su11133695.

Idris, M. S., K. S. Jean, and R. Zakariya. 2009. "Hyperspectral Discrimination and Separability Analysis of Coral Reef Communities in Redang Island." *Journal of Sustainability Science and Management* 4 (2): 36–43.

Joyce, K. E., and S. R. Phinn. 2003. "Hyperspectral Analysis of Chlorophyll Content and Photosynthetic Capacity of Coral Reef Substrates." *Limnology and Oceanography* 48 (1part2): 489–496. doi:10.4319/lo.2003.48.1_part_2.0489.

Karpouzli, E., and T. Malthus, 2003. Hyperspectral discrimination of coral reef benthic communities, Igarss 2003: Ieee International Geoscience and Remote Sensing Symposium, Vols I - Vii, Proceedings: Learning from Earth's Shapes and Sizes, New York: Ieee.

Karpouzli, E., T. J. Malthus, and C. J. Place. 2004. "Hyperspectral Discrimination of Coral Reef Benthic Communities in the Western Caribbean." *Coral Reefs* 23 (1): 141–151. doi:10.1007/s00338-003-0363-9.

Kazama, Y., and T. Yamamoto. 2017. "Shallow Water Bathymetry Correction Using Sea Bottom Classification with Multispectral Satellite Imagery." Vol. 10422, SPIE Remote Sensing: SPIE.

Klemas, V. 2011. "Remote Sensing Techniques for Studying Coastal Ecosystems: An Overview." *Journal of Coastal Research* 27 (1): 2–17. doi:10.2112/jcoastres-d-10-00103.1.

Knudby, A., E. LeDrew, and C. Newman. 2007. "Progress in the Use of Remote Sensing for Coral Reef Biodiversity Studies." *Progress in Physical Geography* 31 (4): 421–434. doi:10.1177/0309133307081292.

Kutser, T., A. G. Dekker, and W. Skirving. 2003. "Modeling Spectral Discrimination of Great Barrier Reef Benthic Communities by Remote Sensing Instruments." *Limnology and Oceanography* 48 (1): 497–510. doi:10.4319/lo.2003.48.1_part_2.0497.

Kutser, T., and D. L. B. Jupp. 2006. "On the Possibility of Mapping Living Corals to the Species Level Based on Their Optical Signatures." *Estuarine, Coastal and Shelf Science* 69 (3): 607–614. doi:10.1016/j.ecss.2006.05.026.

Kutser, T., I. Miller, and D. L. B. Jupp. 2006. "Mapping Coral Reef Benthic Substrates Using Hyperspectral Space-borne Images and Spectral Libraries." *Estuarine, Coastal and Shelf Science* 70 (3): 449–460. doi:10.1016/j.ecss.2006.06.026.

Kutser, T., W. Skirving, J. Parslow, L. Clementson, T. Done, M. Wakeford, and I. Miller. 2001. Spectral discrimination of coral reef bottom types, Igarss 2001: Scanning the Present and Resolving the Future, Vols 1-7, Proceedings, New York: Ieee.

Leiper, I., S. Phinn, and A. G. Dekker. 2012. "Spectral Reflectance of Coral Reef Benthos and Substrate Assemblages on Heron Reef, Australia." *International Journal of Remote Sensing* 33 (12): 3946–3965. doi:10.1080/01431161.2011.637675.

Lesser, M. P., and C. D. Mobley. 2007. "Bathymetry, Water Optical Properties, and Benthic Classification of Coral Reefs Using Hyperspectral Remote Sensing Imagery." *Coral Reefs* 26 (4): 819–829. doi:10.1007/s00338-007-0271-5.

Li, J. W., N. S. Fabina, D. E. Knapp, and G. P. Asner. 2020. "The Sensitivity of Multi-spectral Satellite Sensors to Benthic Habitat Change." *Remote Sensing* 12 (3): 20. doi:10.3390/rs12030532.

Lyzenga, D. R. 1978. "Passive Remote-sensing Techniques for Mapping Water Depth and Bottom Features." *Applied Optics* 17 (3): 379–383. doi:10.1364/ao.17.000379.

Maritorena, S., A. Morel, and B. Gentili. 1994. "Diffuse Reflectance of Oceanic Shallow Waters: Influence of Water Depth and Bottom Albedo." *Limnology and Oceanography* 39 (7): 1689–1703. doi:10.4319/lo.1994.39.7.1689.

Mazel, C. H. 1995. "Spectral Measurements of Fluorescence Emission in Caribbean Cnidarians." *Marine Ecology Progress Series* 120 (1–3): 185–191. doi:10.3354/meps120185.

Miller, I., B. C. Forster, S. W. Laffan, and R. W. Brander. 2016. "Bidirectional Reflectance of Coral Growth-forms." *International Journal of Remote Sensing* 37 (7): 1553–1567. doi:10.1080/01431161.2016.1154220.

Minghelli-Roman, A., J. R. Chisholm, M. Marchioretti, and J. M. Jaubert. 2002. "Discrimination of Coral Reflectance Spectra in the Red Sea." *Coral Reefs* 21 (3): 307–314. doi:10.1007/s00338-002-0249-2.

Mishra, D. R., S. Narumalani, D. Rundquist, M. Lawson, and R. Perk. 2007. "Enhancing the Detection and Classification of Coral Reef and Associated Benthic Habitats: A Hyperspectral Remote Sensing Approach." *Journal of Geophysical Research-Oceans* 112 (C8): 18. doi:10.1029/2006jc003892.

Mobley, C. D. 1994. "*Light and Water: Radiative Transfer in Natural Waters*." San Diego: Academic Press.

Mobley, C. D., L. K. Sundman, C. O. Davis, J. H. Bowles, T. V. Downes, R. A. Leathers, M. J. Montes, et al. 2005. "Interpretation of Hyperspectral Remote-sensing Imagery by Spectrum Matching and Look-up Tables." *Applied Optics* 44 (17): 3576–3592. doi:10.1364/AO.44.003576.

Morel, A., and R. C. Smith. 1982. "Terminology and Units in Optical Oceanography." *Marine Geodesy* 5 (4): 335–349. doi:10.1080/15210608209379431.

Mueller, J. L., A. Morel, R. Frouin, C. Davis, R. Arnone, K. Carder, Z. P. Lee, R. G. Steward, S. Hooker, and C. D. Mobley. 2003. "Ocean Optics Protocols for Satellite Ocean Color Sensor Validation, Revision 4. Volume III: Radiometric Measurements and Data Analysis Protocols."

Mumby, P. J., E. P. Green, C. D. Clark, and A. J. Edwards. 1998. "Digital Analysis of Multispectral Airborne Imagery of Coral Reefs." *Coral Reefs* 17 (1): 59–69. doi:10.1007/s003380050096.

Myers, M. R., J. T. Hardy, C. H. Mazel, and P. Dustan. 1999. "Optical Spectra and Pigmentation of Caribbean Reef Corals and Macroalgae." *Coral Reefs* 18 (2): 179–186. doi:10.1007/s003380050177.

Niedzwiedzki, D. M., J. Jiang, C. S. Lo, and R. E. Blankenship. 2014. "Spectroscopic Properties of the Chlorophyll a–Chlorophyll c2–Peridinin-Protein-Complex (Acppc) from the Coral Symbiotic Dinoflagellate Symbiodinium." *Photosynthesis Research* 120 (1): 125–139. doi:10.1007/s11120-013-9794-5.

Niroumand-Jadidi, M., N. Pahlevan, and A. Vitti. 2019. "Mapping Substrate Types and Compositions in Shallow Streams." *Remote Sensing* 11 (3): 21. doi:10.3390/rs11030262.

Petit, T., T. Bajjouk, P. Mouquet, S. Rochette, B. Vozel, and C. Delacourt. 2017. "Hyperspectral Remote Sensing of Coral Reefs by Semi-analytical Model Inversion - Comparison of Different Inversion Setups." *Remote Sensing of Environment* 190: 348–365. doi:10.1016/j.rse.2017.01.004.

Roelfsema, C. M., and S. R. Phinn. 2012. "Spectral Reflectance Library of Selected Biotic and Abiotic Coral Reef Features in Heron Reef." Pangaea. (Dataset) doi: 10.1594/PANGAEA.804589

Ruffin, C., R. L. King, and N. H. Younan. 2008. "A Combined Derivative Spectroscopy and Savitzky-Golay Filtering Method for the Analysis of Hyperspectral Data." *GIScience and Remote Sensing* 45 (1): 1–15. doi:10.2747/1548-1603.45.1.1.

Russell, B. J., H. M. Dierssen, T. C. LaJeunesse, K. D. Hoadley, M. E. Warner, D. W. Kemp, and T. G. Bateman. 2016. "Spectral Reflectance of Palauan Reef-Building Coral with Different Symbionts in Response to Elevated Temperature." *Remote Sensing* 8 (3): 164. doi:10.3390/rs8030164.

Savitzky, A., and M. J. E. Golay. 1964. "Smoothing and Differentiation of Data by Simplified Least Squares Procedures." *Analytical Chemistry* 36 (8): 1627–1639. doi:10.1021/ac60214a047.

Stambler, N., and N. Shashar. 2007. "Variation in Spectral Reflectance of the Hermatypic Corals, Stylophora Pistillata and Pocillopora Damicornis." *Journal of Experimental Marine Biology and Ecology* 351 (1–2): 143–149. doi:10.1016/j.jembe.2007.06.014.

Torres-Perez, J. L., L. S. Guild, and R. A. Armstrong. 2012. "Hyperspectral Distinction of Two Caribbean Shallow-Water Corals Based on Their Pigments and Corresponding Reflectance." *Remote Sensing* 4 (12): 3813–3832. doi:10.3390/rs4123813.

Torres-Perez, J. L., L. S. Guild, R. A. Armstrong, J. Corredor, A. Zuluaga-Montero, R. Polanco, and W. I. L. Davies. 2015. "Relative Pigment Composition and Remote Sensing Reflectance of Caribbean Shallow-Water Corals." *Plos One* 10 (11): 20. doi:10.1371/journal.pone.0143709.

Wettle, M., G. Ferrier, A. J. Lawrence, and K. Anderson. 2003. "Fourth Derivative Analysis of Red Sea Coral Reflectance Spectra." *International Journal of Remote Sensing* 24 (19): 3867–3872. doi:10.1080/0143116031000075945.

Wicaksono, P., M. A. Fauzan, I. S. W. Kumara, R. N. Yogyantoro, W. Lazuardi, and Z. Zhafarina. 2019. "Analysis of Reflectance Spectra of Tropical Seagrass Species and Their Value for Mapping Using Multispectral Satellite Images." *International Journal of Remote Sensing* 40 (23): 8955–8978. doi:10.1080/01431161.2019.1624866.

Yamano, H., M. Tamura, Y. Kunii, and M. Hidaka. 2002. "Hyperspectral Remote Sensing and Radiative Transfer Simulation as a Tool for Monitoring Coral Reef Health." *Marine Technology Society Journal* 36 (1): 4–13. doi:10.4031/002533202787914205.

Yamano, H., M. Tamura, Y. Kunii, and M. Hidaka. 2003. "Spectral Reflectance as a Potential Tool for Detecting Stressed Corals." *Journal of the Japanese Coral Reef Society* 5 (5): 1–10. doi:10.3755/jcrs.2003.1.

Zeng, K., X. Zhan-tang, Y.-Z. Yang, Y. Zhang, W. Zhou, L. Cai, and H. Huang. 2020. "Design and Application of Reflectance Measurement System for Sea Bottom in Optically Shallow Water." *Spectroscopy and Spectral Analysis* 40 (2): 579–585. doi:10.3964/j.1000-0593(2020)02-0579-07.

Zhao, M., K.-F. Yu, and Q. Zhang. 2006. "Review on Coral Reefs Biodiversity and Ecological Function." *Acta Ecologica Sinica* 26: 186–194.

Zoffoli, M. L., R. Frouin, and M. Kampel. 2014. "Water Column Correction for Coral Reef Studies by Remote Sensing." *Sensors* 14 (9): 16881–16931. doi:10.3390/s140916881.